Singlet-octet mixing of scalar mesons in a generalized Nambu–Jona-Lasinio model

L. S. Celenza, Xiang-Dong Li, and C. M. Shakin*
Department of Physics and Center for Nuclear Theory, Brooklyn College of the City University of New York, Brooklyn, New York 11210
(Received 19 June 1997)

We study the nonstrange scalar-isoscalar states of a generalized Nambu–Jona-Lasinio model that includes the 't Hooft interaction and a model of confinement. We also include coupling of the $q\bar{q}$ states to the two-pion continuum in our analysis. (Our study is limited to energies $q^2 \leqslant 1.8\ \mathrm{GeV}^2$, since to go beyond $q^2 = 2.0\ \mathrm{GeV}^2$ we need to change our method of calculation.) After introducing octet-singlet mixing we find two states, σ_1 and σ_2, at energies of 1.00 and 1.28 GeV, respectively. The first of these is predominantly a SU(3) singlet, while the second state is rather strongly mixed. Of particular interest for nuclear physics is the behavior of the quark-quark T matrix for small spacelike values of q^2. Because of a strong q^2 dependence of the T matrix at the opening of the two-pion continuum at $q^2 = 4m_\pi^2$, the *effective* mass that parametrizes scalar-isoscalar exchange in the T matrix is about 520 MeV. Thus, in a model of the nucleon-nucleon interaction, whose ingredients are a T matrix for the interaction of off-mass-shell quarks and valence-quark nucleon form factors, we can provide a basis for the use of a low-mass *effective* σ meson in nuclear physics. [S0556-2813(97)02112-2]

PACS number(s): 24.85.+p, 12.39.−x, 13.75.Cs, 21.30.Fe

I. INTRODUCTION

In a recent work we studied the properties of the σ meson in a generalized Nambu–Jona-Lasinio (NJL) model with SU(2)-flavor symmetry [1]. Our generalized model contains a model of confinement which is used in the calculation of loop integrals. The confinement model serves to eliminate unphysical cuts that would arise if the quark and antiquark were to both go on their positive mass shells [2]. That feature allows us to use the model at energies larger than those we could consider in the absence of a confinement model. The introduction of a confinement model also allows us to make use of dispersion relations in which the discontinuities are across cuts that arise when *hadrons* go on mass shell [1].

In this work we wish to extend our considerations to a NJL model with SU(3) flavor symmetry and with the 't Hooft interaction added. Important theoretical developments and various applications of that model may be found in Refs. [3–7], while useful reviews appear in Refs. [8–10]. Our motivation in studying the SU(3)-flavor version of the NJL model has its origin in some of our earlier work using the SU(2) version of that model [11]. There we found that the quark-quark T matrix that describes scalar-isoscalar exchange could be well approximated by the exchange of an *effective* σ meson of mass of about 500 MeV, if q^2 was small and spacelike. That result allowed us to understand some aspects of the one-boson-exchange model of the nucleon-nucleon interaction [12] in the case of scalar-isoscalar exchange. (Since we had used constituent quark masses of about 260 MeV in our earlier work, our result might not be all that surprising.) It is of interest to see if our result for the mass of the *effective* σ is maintained if we use larger constituent quark masses and the SU(3)-flavor version of the NJL model. Thus, we are here more interested in the behavior of the quark-quark T matrix for small q^2 than in the spectroscopy in the region of 1 GeV, where the *physical* σ meson is to be found.

In a previous work dealing with the octet of pseudoscalar mesons and the η' we studied η^0-η^8 mixing which gives rise to the physical states η and η' [13]. When we consider scalar mesons, the analogous problem is the mixing of σ^0 (singlet) with σ^8 (octet) states to yield the physical states which we denote as $\sigma_1, \sigma_2, \ldots$. Here, σ_1 has the lowest energy and is predominantly the $\sigma^0(1P)$. It is found that the next state σ_2 is rather strongly mixed. Note that in the case of η^0-η^8 mixing, it is the η' that is predominantly the singlet state. These features are characteristic of the 't Hooft interaction [14].

The use of the SU(3)-flavor NJL model and the 't Hooft interaction to study the scalar octet and the scalar singlet has been described in Ref. [14], where an extensive discussion of the experimental data for scalar meson spectroscopy is presented. In Ref. [14], the states considered have energies equal to or greater than 1 GeV, so that one may question the use of the NJL model (without confinement) to describe the scalar mesons. This problem is avoided in Ref. [14], since the energies of the scalar states are calculated using a bosonization procedure. That procedure is essentially a low-energy (or low-momentum) expansion. Therefore, in such an expansion one stays below the unitarity cuts whose thresholds are given in terms of the constituent quark masses. These thresholds are at $q^2 = (2m_u)^2$, $q^2 = (m_u + m_s)^2$, and $q^2 = (2m_s)^2$ in a model without confinement. One advantage of the methods we use in our work is that we can obtain both the energy and the width of the various mesonic states, since we are able to implement our program at fairly large values of q^2 (with $q^2 > 0$).

A useful approach to the problem of meson mixing is to study a quark-quark T matrix. When calculating the T matrix, one sums various t-channel exchange diagrams. If the T matrix is real, a single mixing angle appears in the formalism when we use an orthogonal transformation to bring the T matrix to diagonal form. (A more elaborate parametrization

*Electronic address: CASBC@CUNYVM.CUNY.EDU

is needed when T is complex.) The relevant equations describing singlet-octet mixing appear in the literature [3–7]. In this work we exhibit these equations modified to include a model of confinement and coupling to the two-pion continuum.

The organization of our work is as follows. In Sec. II we describe some characteristics of our generalized NJL model and describe how we implement our model of confinement. In Sec. III we discuss the calculation of vacuum polarization diagrams that involve a quark and an antiquark. In Sec. IV we describe the formalism used in the calculation of σ^0-σ^8 mixing. In Sec. V we describe the important role played by the coupling of $q\overline{q}$ states to the two-pion continuum. Numerical results are presented in Sec. VI. In Sec. VII we describe the dynamical origin of a low-mass (effective) σ meson for nuclear physics studies. The exchange of this *effective* meson is shown to provide a good representation of the quark-quark T matrix, if the exchanged momentum is spacelike ($q^2 \leqslant 0$). Finally, Sec. VIII contains some further discussion and some conclusions.

II. A GENERALIZED NAMBU–JONA-LASINIO MODEL WITH A MODEL OF CONFINEMENT

In this section we introduce various vacuum polarization integrals that are an essential feature of the NJL model [8–10]. We will then show how the introduction of a model of confinement removes unphysical $q\overline{q}$ cuts from the various loop integrals studied. In Sec. V we will also discuss the coupling of the $q\overline{q}$ states to the two-pion continuum. (It is this feature that gives rise to the large widths obtained for the scalar states in some cases.)

In the past, we have studied the SU(2)-flavor version of the NJL model. Here we consider the SU(3)-flavor version of the model, supplemented by the 't Hooft interaction. The Lagrangian we consider is

$$\mathcal{L}=\overline{q}(i\partial\!\!\!/-m^0)q+G_s\sum_{i=0}^{8}\left[\left(\overline{q}\frac{\lambda^i}{2}q\right)^2+\left(\overline{q}i\gamma_5\frac{\lambda^i}{2}q\right)^2\right]$$

$$+\frac{G_D}{2}\{\det[\overline{q}(1+\gamma_5)q]+\det[\overline{q}(1-\gamma_5)q]\}+\mathcal{L}_{\rm conf}, \tag{2.1}$$

where the λ^i $(i=1,\ldots,8)$ are the Gell-Mann matrices in flavor space and $\lambda^0=(\frac{2}{3})^{1/2}\mathbb{I}$, with $\mathbb{I}$ being the unit matrix. In Eq. (2.1), m^0 denotes a quark mass matrix with diagonal elements, m_u^0, m_d^0, m_s^0. Here, we take $m_u^0=m_d^0=5.5$ MeV and $m_s^0=132$ MeV, which are the values used in Ref. [8]. Further,

$$\mathcal{L}_{\rm conf}=\int d^4y\,\overline{q}(x)\gamma^\mu q(x)V^C(x-y)\overline{q}(y)\gamma_\mu q(y). \tag{2.2}$$

This represents a Lorentz-vector confinement model [1]. For calculations made in Minkowski momentum space, we neglect any dependence of V^C on energy transfer. That is, $V^C(x-y)$ contains a δ function that serves to equate the times associated with points x and y in Eq. (2.2). We use $V^C(r)=\kappa r\,\exp(-\mu r)$, where κ is the ''string tension'' and μ is a small parameter used to soften the singularities of the Fourier transform of $V^C(r)$. The Fourier transform of $V^C(r)$ is then

$$V^C(\vec{k}-\vec{k}')=-8\pi\kappa\left[\frac{1}{[(\vec{k}-\vec{k}')^2+\mu^2]^2}-\frac{4\mu^2}{[(\vec{k}-\vec{k}')^2+\mu^2]^3}\right]. \tag{2.3}$$

We have used $\mu=0.020$ GeV, and for the Lorentz-vector confinement model of Eq. (2.2), we use $\kappa=0.05$ GeV^2.

Another confinement model is the V-A model that we have used in some of our earlier work [15]. In that model

$$\mathcal{L}_{\rm conf}(x)=\int d^4y[\overline{q}(x)\gamma^\mu q(x)V^C(x-y)\overline{q}(y)\gamma_\mu q(y)$$

$$-\overline{q}(x)\gamma^\mu\gamma_5 q(x)V^C(x-y)\overline{q}(y)\gamma_\mu\gamma_5 q(y)]. \tag{2.4}$$

In order to describe how confinement is introduced in the model, we refer to Fig. 1. There, the filled triangular region denotes a vertex operator that is defined in terms of the confinement interaction $V^C(\vec{k}\text{-}\vec{k}')$, shown as a dashed line. [Note that the vertex $\Gamma_S(q,k)$ satisfies an inhomogeneous equation.] Since we do not study strange mesons in this work, we may limit ourselves to the case where the flavor of the quark and antiquark at the vertex is the same. The V-A

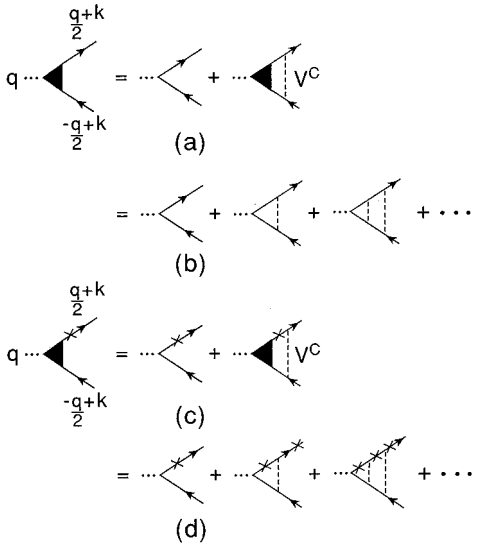

FIG. 1. (a) The diagram represents the equation for the vertex $\Gamma_S(q,k)$, which serves to represent a sum of a series of confining interactions. These interactions are shown here as dashed lines. (b) A perturbative expansion for $\Gamma_S(q,k)$ is shown. (c) The vertex $\Gamma^{+-}(q,k)$ is obtained in our analysis when the quark is on its positive mass shell. (Here the cross denotes a quark on its positive mass shell.) (d) A perturbative expansion for $\Gamma^{+-}(q,k)$ is shown. The dashed line introduces a factor $-iV^C(k-k')\gamma^\mu(1)\gamma_\mu(2)$ when applying the Feynman rules in the evaluation of the diagrams.

model leads to a particularly simple result $\overline{\Gamma_S}(q,k) = \mathbb{I}\Gamma_S(q,k)$, where $\mathbb{I}$ denotes the unit matrix in flavor space and in the space of Dirac matrices, and where $\Gamma_S(q,k)$ is a scalar function [15]. This scalar function has a very important property. It is equal to zero when the quark and the antiquark both go on their positive mass shells. It is that feature that eliminates unphysical $q\overline{q}$ cuts from the various functions that arise upon performing loop integrals.

The situation in the case of Lorentz-vector confinement is more complicated since $\overline{\Gamma_S}(q,k)$ then contains several terms having different Dirac matrix structure. In that case it is useful to introduce the projection operators

$$\Lambda^{(+)}(\vec{k}) = \frac{\not{k}+m}{2m}, \tag{2.5}$$

with $k^\mu = [E(\vec{k}),\vec{k}]$ and

$$\Lambda^{(-)}(-\vec{k}) = \frac{\not{\tilde{k}}+m}{2m}, \tag{2.6}$$

with $\tilde{k}^\mu = [-E(\vec{k}),\vec{k}]$. Here $E(\vec{k}) = [\vec{k}^2+m^2]^{1/2}$. In this case, we may define functions $\Gamma^{-+}(q,k)$, $\Gamma^{+-}(q,k)$, etc.:

$$\Lambda^{(+)}(\vec{k})\overline{\Gamma_S}(q,k)\Lambda^{(-)}(-\vec{k}) = \Gamma^{+-}(q,k)\Lambda^{(+)}(\vec{k})\Lambda^{(-)}(-\vec{k}), \tag{2.7}$$

$$\Lambda^{(-)}(-\vec{k})\overline{\Gamma_S}(q,k)\Lambda^{(+)}(\vec{k}) = \Gamma^{-+}(q,k)\Lambda^{(-)}(-\vec{k})\Lambda^{(+)}(\vec{k}), \tag{2.8}$$

$$\Lambda^{(+)}(\vec{k})\overline{\Gamma_S}(q,k)\Lambda^{(+)}(\vec{k}) = \Gamma^{++}(q,k)\Lambda^{(+)}(\vec{k}), \tag{2.9}$$

and

$$\Lambda^{(-)}(-\vec{k})\overline{\Gamma_S}(q,k)\Lambda^{(-)}(-\vec{k}) = \Gamma^{--}(q,k)\Lambda^{(-)}(-\vec{k}). \tag{2.10}$$

In Ref. [13] we described the calculation of the various functions that appear in Eqs. (2.7)–(2.10). We also demonstrated how these functions are used in the calculation of loop integrals. In the next section we discuss their use in the calculation of $q\overline{q}$ vacuum-polarization diagrams that are needed in our work.

III. VACUUM-POLARIZATION INTEGRALS

Here we consider the calculation of the diagrams of Fig. 2(c). A more comprehensive discussion is given in Ref. [13], so that our discussion here is limited to a short review. The basic integral for a quark and antiquark of a single flavor is obtained from the evaluation of the diagram shown in Fig. 2(b). We have

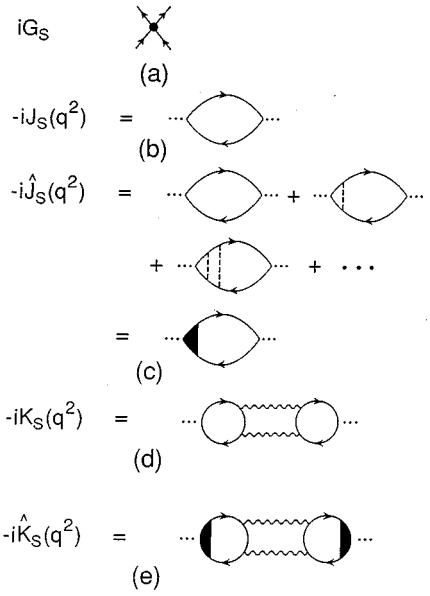

FIG. 2. (a) The zero-range two-quark interaction of the NJL model is shown. (b) The quark-loop integral in the scalar-isoscalar channel is shown. (c) The quark-loop integral that includes a ladder of confining interactions (dashed lines) is shown. The filled triangular region denotes the vertex function that serves to sum the ladder of confining interactions. (d) The function $K_S(q^2)$ describes the effects of coupling to the two-pion continuum. [See Sec. V.] (e) The function $\hat{K}_S(q^2)$ includes two confinement vertex functions and has a cut for $q^2 > 4m_\pi^2$.

$$-iJ(q^2) = (-1)n_c\mathrm{Tr}\int \frac{d^4k}{(2\pi)^4} iS(q/2+k)iS(-q/2+k), \tag{3.1}$$

where $S(p) = [\not{p}-m+i\epsilon]^{-1}$ is the quark propagator and m is the constituent quark mass. The introduction of confinement proceeds via the definition

$$-i\hat{J}(q^2) = n_c\mathrm{Tr}\int \frac{d^4k}{(2\pi)^4} S(q/2+k)\overline{\Gamma_S}(q,k)S(-q/2+k), \tag{3.2}$$

where $\overline{\Gamma_S}(q,k)$ is represented by the filled triangular area in Fig. 2(c). In the calculation of $\hat{J}(q^2)$ it is useful to introduce the representation

$$S(k) = \frac{m}{E(\vec{k})}\left[\frac{\Lambda^{(+)}(\vec{k})}{k^0-E(\vec{k})+i\epsilon} - \frac{\Lambda^{(-)}(-\vec{k})}{k^0+E(\vec{k})-i\epsilon}\right], \tag{3.3}$$

and work in the frame where $\vec{q}=0$. Thus,

$$-i\hat{J}(q^2)=-n_c\mathrm{Tr}\int\frac{d^4k}{(2\pi)^4}\frac{m}{E(\vec{k})}\left[\frac{\Lambda^{(+)}(\vec{k})\overline{\Gamma_S}(q,k)\Lambda^{(-)}(-\vec{k})}{[q^0/2+k^0-E(\vec{k})+i\epsilon][-q^0/2+k^0+E(\vec{k})-i\epsilon]}\right.$$
$$\left.+\frac{\Lambda^{(-)}(-\vec{k})\overline{\Gamma_S}(q,k)\Lambda^{(+)}(\vec{k})}{[q^0/2+k^0+E(\vec{k})-i\epsilon][-q^0/2+k^0-E(\vec{k})+i\epsilon]}\right], \tag{3.4}$$

where m denotes the constituent quark mass. We proceed by evaluating the integral in the lower half of the complex k^0 plane. There are two contributions in which either the quark goes on its *positive* mass shell or the antiquark goes on its *negative* mass shell [16]. Thus, when $\Gamma^{+-}(q,k)$ appears in the final result, it has the quark on its positive mass shell and we write $\Gamma^{+-}(q^0,|\vec{k}|)$ for this function in the frame where $\vec{q}=0$. On the other hand, $\Gamma^{-+}(q^0,|\vec{k}|)$ has the antiquark on its *negative* mass shell in the final result. When we neglected energy transfer in the confining interaction, we found that $\Gamma^{+-}(q^0,|\vec{k}|)=\Gamma^{-+}(q^0,|\vec{k}|)$ and $\Gamma^{++}(q^0,|\vec{k}|)=\Gamma^{--}(q^0,|\vec{k}|)$ for the case of vector confinement [1]. In Figs. 3 and 4 we show values obtained for $\Gamma^{+-}(q^0,|\vec{k}|)$ and $\Gamma^{++}(q^0,|\vec{k}|)$ in Ref. [1], where we used a smaller constituent quark mass for the up and down quarks than that used here. (Here we use $m_u=m_d=364$ MeV and $m_s=522$ MeV.)

In the evaluation of the various functions $\hat{J}(q^2)$, we require a cutoff for the integral over $\vec{k}$. We choose $|\vec{k}|\leq\Lambda_3$, where Λ_3 is chosen such that the values for the condensates are the same as those presented in Ref. [8]. There, a Euclidean momentum space cutoff of $\Lambda_E=0.90$ GeV was used. We found that we should put $\Lambda_3=0.622$ GeV on the basis of this procedure.

It is important to understand that there are solutions of equation for $\overline{\Gamma_S}(q,k)$ when we drop the driving term. The solutions of the resulting (homogeneous) equation are just the vertex functions of the bound states in the confining potential. Since such states are present, $\overline{\Gamma_S}(q,k)$ will have poles at $q^2=M_i^2$ where the M_i are the mass parameters for the bound states in the confining field. Therefore, $\hat{J}(q^2)$ will also have poles at $q^2=M_i^2$.

IV. COUPLED CHANNEL DYNAMICS FOR σ^0-σ^8 MIXING

Here we study the quark-quark T matrix that describes scalar-isoscalar exchange. We generalize the equations presented in Refs. [3–7] to include confinement and coupling to the two-pion continuum. It is useful to define effective coupling constants

$$G_{00}^S=\frac{1}{2}(G_S-G_Dc_{00}), \tag{4.1}$$

$$G_{88}^S=\frac{1}{2}(G_S-G_Dc_{88}), \tag{4.2}$$

$$G_{08}^S=-\frac{1}{2}G_Dc_{08}, \tag{4.3}$$

where

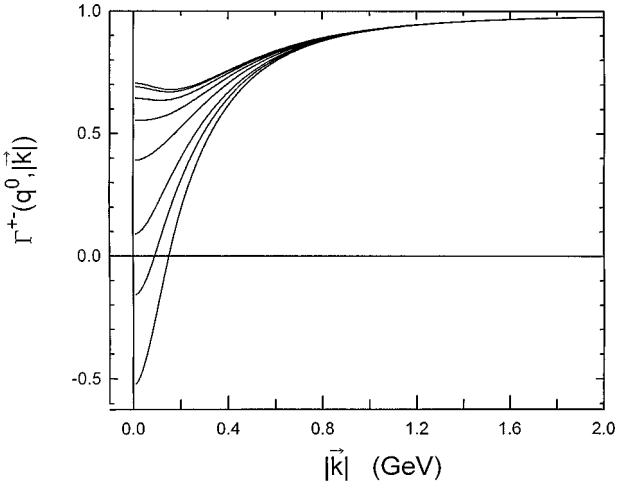

FIG. 3. Values of $\Gamma^{+-}(q^0,|\vec{k}|)$ are shown. Starting from the uppermost curve and moving downward, the values of q^0 are 0, 0.10, 0.20, 0.30, 0.40, 0.50, 0.55, and 0.60 MeV. For the last two of these curves, $\Gamma^{+-}(q^0,|\vec{k}_{\rm on}|)=0$. Here $\vec{k}_{\rm on}^2=(q_0/2)^2-m_q^2$, $m_q=0.260$ GeV, $\mu=0.030$ GeV, and $\kappa=0.05$ GeV^2. (This figure appears as Fig. 2 of Ref. [1].)

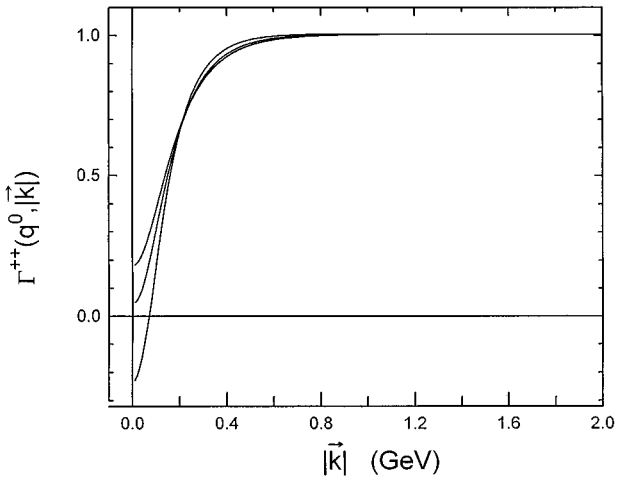

FIG. 4. Values of $\Gamma^{++}(q^0,|\vec{k}|)$ are shown. Starting with the uppermost curve and moving downward, the values of q^0 are 0, 0.4, and 0.6 GeV. Here $m_q=0.260$ GeV, $\mu=0.030$ GeV, and $\kappa=0.05$ GeV^2. (This figure appears as Fig. 3 of Ref. [1].)

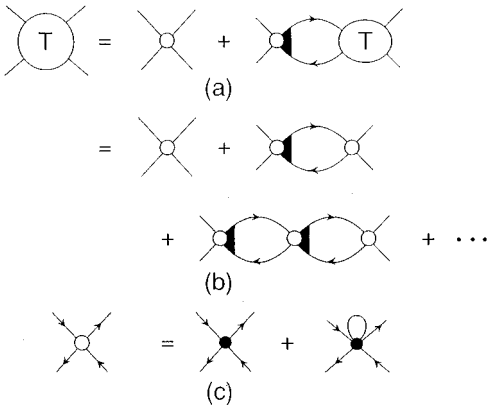

FIG. 5. (a) The equation for the quark-antiquark T matrix is shown for the case $\hat{K}_S(q^2)=0$. The circle is the effective interaction. [See Eqs. (4.1)–(4.3) and (c) below.] The filled triangular region denotes the vertex for the confining interaction. (b) An expansion of the T matrix is given in terms of the effective interaction (circle) and the vacuum-polarization integrals $\hat{J}(q^2)$. (c) The effective interaction (open circle) is composed of the original (two-quark) NJL interaction and the three-quark 't Hooft interaction.

$$c_{00}=-\frac{2}{3}\,(2\langle\overline{uu}\rangle+\langle\overline{ss}\rangle), \tag{4.4}$$

$$c_{88}=\frac{1}{3}\,(4\langle\overline{uu}\rangle-\langle\overline{ss}\rangle), \tag{4.5}$$

and

$$c_{08}=\frac{\sqrt{2}}{3}\,(\langle\overline{uu}\rangle-\langle\overline{ss}\rangle). \tag{4.6}$$

[See Fig. 5.] In this work we do not introduce any new parameters. The parameter values are taken from Ref. [1] and, except for G_S, they are the same as those given in Ref. [8]. We have $G_S=21.53\ \mathrm{GeV}^{-2}$, $G_D=-239.1\ \mathrm{GeV}^{-5}$, $\langle\overline{uu}\rangle=\langle\overline{dd}\rangle=-(0.248\ \mathrm{GeV})^3=-0.01525\ \mathrm{GeV}^3$, and $\langle\overline{ss}\rangle=-(0.258\ \mathrm{GeV})^3=-0.01717\ \mathrm{GeV}^3$. Recall that we also use $m_u^0=m_d^0=5.5$ MeV, $m_s^0=132$ MeV, $m_u=m_d=364$ MeV, and $m_s=522$ MeV.

It is useful to introduce a set of functions defined in terms of the functions defined previously,

$$\hat{J}_{00}(q^2)=\frac{2}{3}\,[\hat{J}_u(q^2)+\hat{J}_d(q^2)+\hat{J}_s(q^2)] \tag{4.7}$$

and

$$\hat{J}_{88}(q^2)=\frac{1}{3}\,[\hat{J}_u(q^2)+\hat{J}_d(q^2)+4\hat{J}_s(q^2)], \tag{4.8}$$

$$\hat{J}_{08}(q^2)=\frac{\sqrt{2}}{3}\,[\hat{J}_u(q^2)+\hat{J}_d(q^2)-2\hat{J}_s(q^2)]. \tag{4.9}$$

We then define the matrices

$$G=\begin{pmatrix} G_{00}^S & G_{08}^S \\ G_{08}^S & G_{88}^S \end{pmatrix}, \tag{4.10}$$

and

$$\hat{J}(q^2)=\begin{pmatrix} \hat{J}_{00}(q^2) & \hat{J}_{08}(q^2) \\ \hat{J}_{08}(q^2) & \hat{J}_{88}(q^2) \end{pmatrix}. \tag{4.11}$$

In the next section we will introduce a set of functions that describe the coupling of the $q\overline{q}$ states to the two-pion continuum. Making use of the functions defined there, we introduce the matrix

$$\hat{K}(q^2)=\begin{pmatrix} \hat{K}_{00}(q^2) & \hat{K}_{08}(q^2) \\ \hat{K}_{08}(q^2) & \hat{K}_{88}(q^2) \end{pmatrix}, \tag{4.12}$$

as well as the matrix

$$\overline{J(q^2)}=\hat{J}(q^2)+\hat{K}(q^2). \tag{4.13}$$

Note that $\hat{K}(q^2)=\mathrm{Re}\hat{K}(q^2)+i\,\mathrm{Im}\hat{K}(q^2)$, with $\mathrm{Im}\hat{K}(q^2)$ equal to zero when $q^2<4m_\pi^2$.

The T matrix, exclusive of Dirac matrices and flavor matrices, then satisfies the matrix equation

$$T(q^2)=-G+G\overline{J(q^2)}T(q^2), \tag{4.14}$$

or

$$T(q^2)=-[\mathbb{I}-G\overline{J(q^2)}]^{-1}G. \tag{4.15}$$

We also introduce the matrix

$$D(q^2)=\mathbb{I}-G\overline{J(q^2)} \tag{4.16}$$

$$=\begin{bmatrix} D_{11}(q^2) & D_{12}(q^2) \\ D_{21}(q^2) & D_{22}(q^2) \end{bmatrix}, \tag{4.17}$$

with

$$D_{11}(q^2)=1-[G_{00}^S\overline{J_{00}}(q^2)+G_{08}^S\overline{J_{08}}(q^2)], \tag{4.18}$$

$$D_{12}(q^2)=-[G_{00}^S\overline{J_{08}}(q^2)+G_{08}^S\overline{J_{88}}(q^2)], \tag{4.19}$$

$$D_{21}(q^2)=-[G_{08}^S\overline{J_{00}}(q^2)+G_{88}^S\overline{J_{08}}(q^2)], \tag{4.20}$$

and

$$D_{22}(q^2)=1-[G_{08}^S\overline{J_{08}}(q^2)+G_{88}^S\overline{J_{88}}(q^2)]. \tag{4.21}$$

With these definitions, we may write

$$T(q^2)=\begin{bmatrix} A_S(q^2) & B_S(q^2) \\ B_S(q^2) & C_S(q^2) \end{bmatrix}, \tag{4.22}$$

with

$$A_S(q^2)=-\frac{1}{\det D(q^2)}\,[G_{00}^S-(G_{88}^SG_{00}^S-G_{08}^SG_{08}^S)\overline{J_{88}}(q^2)], \tag{4.23}$$

$$B_S(q^2)=-\frac{1}{\det D(q^2)}\,[G_{08}^S-(G_{08}^SG_{08}^S-G_{00}^SG_{88}^S)\overline{J_{08}}(q^2)], \tag{4.24}$$

and

$$C_S(q^2) = -\frac{1}{\det D(q^2)}\,[G^S_{88} - (G^S_{00}G^S_{88} - G^S_{08}G^S_{08})\overline{J_{00}}(q^2)]. \tag{4.25}$$

Note that in the absence of octet-singlet coupling [$G^S_{08} = \overline{J_{08}}(q^2) = 0$], we have $B_S(q^2) = 0$,

$$A_S(q^2) = -\frac{G^S_{00}}{1 - G^S_{00}\overline{J_{00}}(q^2)} \tag{4.26}$$

and

$$C_S(q^2) = -\frac{G^S_{88}}{1 - G^S_{88}\overline{J_{88}}(q^2)}. \tag{4.27}$$

If we use Eq. (4.26), we see that the masses of the scalar singlet mesons are given by the solution of the equation

$$(G^S_{00})^{-1} - \mathrm{Re}\overline{J_{00}}(m^2_{\sigma^0}) = 0. \tag{4.28}$$

Similarly, we have for the mass of the scalar octet mesons, the solution of the equation

$$(G^S_{88})^{-1} - \mathrm{Re}\overline{J_{88}}(m^2_{\sigma^8}) = 0. \tag{4.29}$$

As we will see, Eqs. (4.28) and (4.29) will have more than one solution.

We note that for $q^2 < 4m^2_\pi$, the T matrix is real. If $q^2 < 4m^2_\pi$, or if we neglect $\mathrm{Im}\hat{K}_S(q^2)$, we can bring T to a diagonal form with a real matrix

$$M(\theta) = \begin{pmatrix} \cos\theta & -\sin\theta \\ \sin\theta & \cos\theta \end{pmatrix}, \tag{4.30}$$

where θ is a function of q^2.

Thus,

$$T_{\mathrm{diag}}(q^2) = M(\theta)T(q^2)M^{-1}(\theta), \tag{4.31}$$

$$= \begin{bmatrix} T_\sigma(q^2) & 0 \\ 0 & T_{\sigma'}(q^2) \end{bmatrix}, \tag{4.32}$$

where

$$T_\sigma(q^2) = A_S(q^2)\cos^2\theta - 2B_S(q^2)\sin\theta\cos\theta + C_S(q^2)\sin^2\theta, \tag{4.33}$$

and

$$T_{\sigma'}(q^2) = A_S(q^2)\sin^2\theta + 2B_S(q^2)\sin\theta\cos\theta + C_S(q^2)\cos^2\theta. \tag{4.34}$$

Alternate expressions for $T_\sigma(q^2)$ and $T_{\sigma'}(q^2)$ that are generally valid are

$$T_\sigma(q^2) = \frac{A_S(q^2) + C_S(q^2)}{2} + \left\{\left[\frac{A_S(q^2) - C_S(q^2)}{2}\right]^2 + B^2_S(q^2)\right\}^{1/2}, \tag{4.35}$$

and

$$T_{\sigma'}(q^2) = \frac{A_S(q^2) + C_S(q^2)}{2} - \left\{\left(\frac{A_S(q^2) - C_S(q^2)}{2}\right)^2 + B^2_S(q^2)\right\}^{1/2}, \tag{4.36}$$

as may be seen by calculating the eigenvalues of the matrix $T(q^2)$ in the case $A_S(q^2)$, $B_S(q^2)$, and $C_s(q^2)$ are complex functions.

We can also see that the matrix $T(q^2)$ takes on a diagonal form when

$$\tan 2\theta(q^2) = \frac{2B_S(q^2)}{C_S(q^2) - A_S(q^2)} \tag{4.37}$$

in the case that $q^2 < 4m^2_\pi$, or if $\mathrm{Im}\hat{K}_S(q^2) = 0$. Equation (4.37), therefore, provides the value of the mixing angle $\theta(q^2)$ for the case in which $A_S(q^2)$, $B_S(q^2)$, and $C_S(q^2)$ are real functions. We find $\theta(q^2) = -12.6^0$ at $q^2 = 0$. (At low energies there is only small singlet-octet mixing.)

It is useful to define the functions $d_\sigma(q^2)$ and $d_{\sigma'}(q^2)$, such that

$$T_\sigma(q^2) = \frac{d_\sigma(q^2)}{\det D(q^2)}, \tag{4.38}$$

and

$$T_{\sigma'}(q^2) = \frac{d_{\sigma'}(q^2)}{\det D(q^2)}. \tag{4.39}$$

If we neglect $\mathrm{Im}\hat{K}_s(q^2)$, or if $q^2 < 4m^2_\pi$, we may find the mass of the resonances that appear in $T_\sigma(q^2)$ or $T_{\sigma'}(q^2)$ from the equation

$$\det D(q^2) = 0. \tag{4.40}$$

In the general case, we can define meson masses by the condition

$$\mathrm{Re}[\det D(q^2)] = 0. \tag{4.41}$$

Equation (4.41) may be used in the presence of octet-singlet mixing and in the case that $\mathrm{Im}\hat{K}_s(q^2)$ is included in the analysis. Note that $\det D(q^2)$ will have a zero at each bound state or resonance. However, in some cases $d_\sigma(q^2)$, or $d_{\sigma'}(q^2)$, may have a corresponding zero such that the resonance is absent from $T_\sigma(q^2)$ or $T_{\sigma'}(q^2)$.

V. COUPLING TO THE TWO-PION CONTINUUM

We presented a detailed discussion of the calculation of $\hat{K}_S(q^2)$ when using the NJL model with SU(2)-flavor symmetry in Ref. [1]. In Fig. 6(a) we exhibit the diagram that

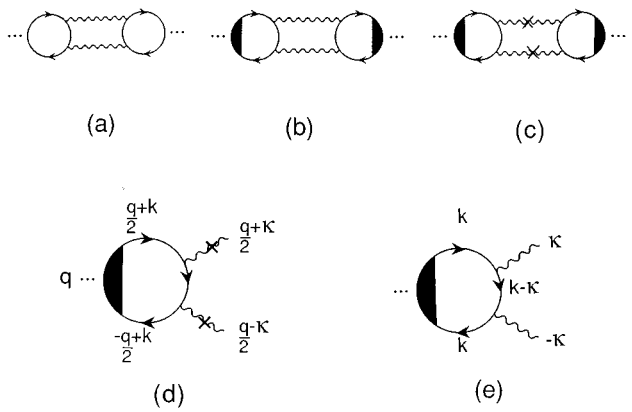

FIG. 6. (a) The diagram represents the function $K_S(q^2)$, which has cuts starting at $q^2=4m_u^2$ and at $q^2=4m_\pi^2$. The wavy lines denote pions. (b) The inclusion of the confining vertex defines the function $\hat{K}_S(q^2)$, which has only one cut starting at $q^2=4m_\pi^2$. (c) The calculation of $\mathrm{Im}\hat{K}_S(q^2)$ may be made by placing the pions on mass shell, as denoted by a cross on the wavy line. (d) A form factor needed in the calculation of the diagram in (c) is shown. (See Ref. [1].) (e) A form factor needed in the calculation of $\hat{K}_S(0)$ is shown. (See Ref. [1].)

defines $K_S(q^2)$ for that theory in the absence of confinement. [Note that for the calculation of $K_S(q^2)$, the flavor matrix at the vertices is the unit matrix.] In Fig. 6(b) we add the confirming vertex, so that the only discontinuity for $K_S(q^2)$ is that across the two-pion cut. We can calculate the discontinuity across the cut by placing the pions on mass shell, as denoted by a cross on the wavy lines in Fig. 6(c). In Fig. 6(d) we show the form factor that has to be calculated when constructing $\mathrm{Im}\hat{K}_S(q^2)$.

In Ref. [1] we saw that we could write a once-subtracted dispersion relation to obtain $\mathrm{Re}\hat{K}_S(q^2)$ from the knowledge of $\hat{K}_S(0)$ and $\mathrm{Im}\hat{K}_S(q^2)$. [The calculation of $\hat{K}_S(0)$ required a separate calculation in which we evaluated the form factor of Fig. 6(e) for the case $q^\mu=0$.] Our results for $\mathrm{Im}\hat{K}_S(0)$ and $\mathrm{Re}\hat{K}_S(q^2)$ are shown in Figs. 7 and 8 [1].

We find that we can calculate the coupling of the $q\overline{q}$ states to the two-pion continuum in the model with SU(3)-flavor symmetry by making use of our earlier calculation. The only modification is the different flavor factors that appear at the vertices. The appropriate definition is then

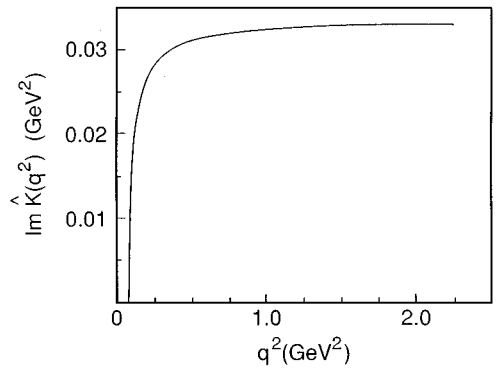

FIG. 7. The function $\mathrm{Im}\hat{K}_S(q^2)$ is shown. This figure appears as Fig. 10 of Ref. [1].

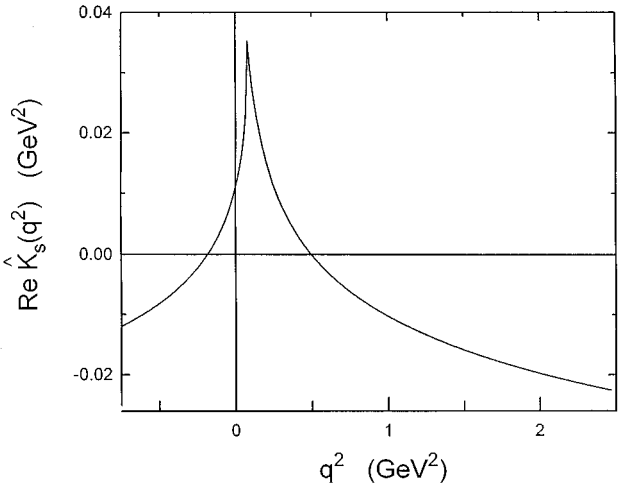

FIG. 8. The function $\mathrm{Re}\hat{K}_S(q^2)$ is shown. The calculation was made using a once-subtracted dispersion relation and a calculated value of $\hat{K}_S(0)$, as described in Ref. [1]. The values of $\mathrm{Im}\hat{K}_S(q^2)$ shown in Fig. 7 were used in the dispersion relation. (See Fig. 11 of Ref. [1].)

$$\hat{K}_{00}(q^2)=\frac{2}{3}\hat{K}_S(q^2), \tag{5.1}$$

$$\hat{K}_{88}(q^2)=\frac{1}{3}\hat{K}_S(q^2), \tag{5.2}$$

and

$$\hat{K}_{08}(q^2)=\frac{\sqrt{2}}{3}\hat{K}_S(q^2). \tag{5.3}$$

Therefore, the matrix $\overline{J(q^2)}=\hat{J}(q^2)+\hat{K}(q^2)$, introduced earlier, has the elements

$$\overline{J_{00}}(q^2)=\frac{2}{3}[\hat{J}_u(q^2)+\hat{J}_d(q^2)+\hat{J}_s(q^2)+\hat{K}_S(q^2)], \tag{5.4}$$

$$\overline{J_{88}}(q^2)=\frac{1}{3}[\hat{J}_u(q^2)+\hat{J}_d(q^2)+4\hat{J}_s(q^2)+\hat{K}_S(q^2)], \tag{5.5}$$

and

$$\overline{J_{08}}(q^2)=\frac{\sqrt{2}}{3}[\hat{J}_u(q^2)+\hat{J}_d(q^2)-2\hat{J}_s(q^2)+\hat{K}_S(q^2)]. \tag{5.6}$$

We have only considered the two-pion cut in the construction of $\mathrm{Im}\hat{K}_S(q^2)$. Other cuts appear in the case of SU(3)-flavor symmetry. However, such cuts appear at higher energy and involve mesons having masses that are significantly larger than the mass of the pion. Their contribution to $\mathrm{Im}\hat{K}_S(q^2)$ is expected to be small.

It can be seen that $\hat{K}_S(q^2)$ only affects singlet states in the absence of singlet-octet coupling. In this model, octet states will take on a width due to their coupling to the singlet states. These comments will be bourne out when we inspect

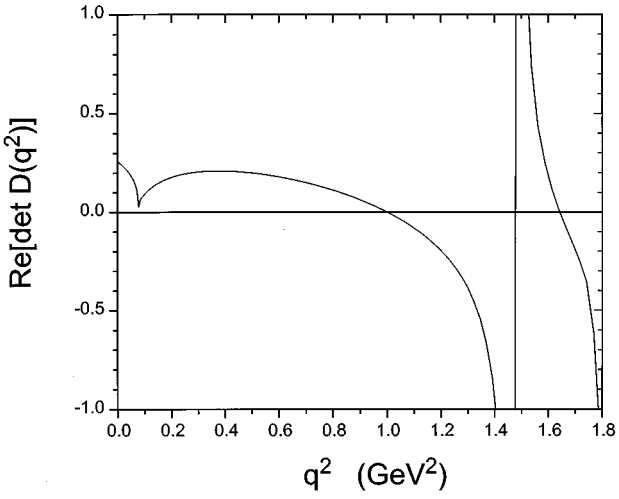

FIG. 9. The figure shows Re[det $D(q^2)$] for the case where both $\mathrm{Re}\hat{K}_S(q^2)$ and $\mathrm{Im}\hat{K}_S(q^2)$ are included, as is singlet-octet coupling. The zeros of this function correspond to the states σ_1 and σ_2. The first of these states is predominantly $\sigma^0(1P)$. (The vertical line shows the position of the singularity at $q^2=1.48\ \mathrm{GeV}^2$ that is due to the presence of a bound state in the confining potential.)

the form of the T matrix in the representation in which it is diagonal. For example, $\mathrm{Re}\hat{K}_S(q^2)$ exhibits strong cusplike behavior near $q^2=4m_\pi^2$. However, that behavior is only reflected in the component of the diagonalized T matrix that we denote as $T_\sigma(q^2)$. That component is predominantly of SU(3)-singlet character since the mixing angle is small in the vicinity of $q^2=0$.

VI. NUMERICAL RESULTS

When we introduce $\mathrm{Im}\hat{K}_S(q^2)$ into our analysis, the functions $A_S(q^2)$, $B_S(q^2)$, and $C_S(q^2)$ become complex. Also, when the T matrix is brought to diagonal form, $T_\sigma(q^2)$ and $T_{\sigma'}(q^2)$ will be complex functions. We begin our analysis by presenting values of Re[det$D(q^2)$] in Fig. 9. The singlet-octet coupling moves two of the four states that originally appeared in the region $q^2\leqslant 1.8\ \mathrm{GeV}$ to higher energy. (The

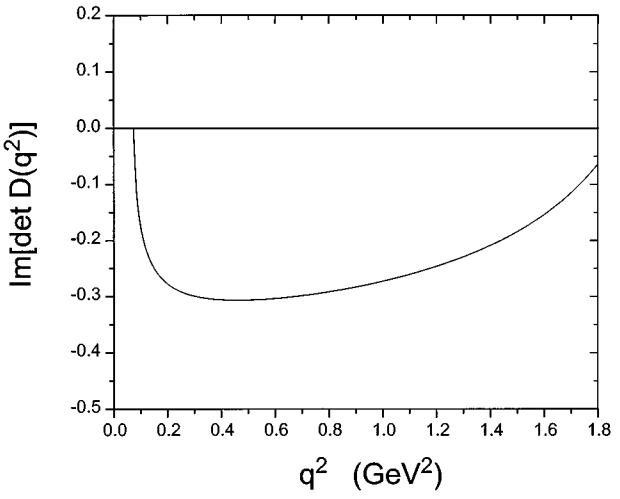

FIG. 10. The figure shows Im[det $D(q^2)$].

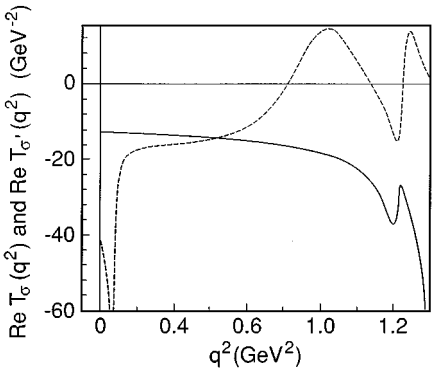

FIG. 11. The figure shows $\mathrm{Re}T_\sigma(q^2)$ (dashed line) and $\mathrm{Re}T_{\sigma'}(q^2)$ (solid line). The cusp behavior for $q^2\simeq 4m_\pi^2$ is only prominent in $\mathrm{Re}T_\sigma(q^2)$. Resonances appear at 1.00 and 1.28 GeV, where $\mathrm{Re}T_\sigma(q^2)$ rises through zero from negative values. [No resonance appears for $\mathrm{Re}T_{\sigma'}(q^2)$ in this energy range.] Note that there is no singularity at $q^2=1.48\ \mathrm{GeV}^2$ in the T matrix.

analysis of Ref. [14] puts the lowest of these states at $q^2\simeq 2.53\ \mathrm{GeV}^2$, which is outside the range of q^2 we are able to investigate in our work.) In Fig. 9 we see cusp behavior at $q^2\equiv 4m_\pi^2$. [The singularity seen in Fig. 9 at $q^2\simeq 1.48\ \mathrm{GeV}^2$ is due to a singularity of $\hat{J}_u(q^2)$. That singularity does not appear in the T matrix elements, as we will see.] Figure 10 shows the values of Im[det$D(q^2)$].

In Fig. 11 we show both $\mathrm{Re}T_\sigma(q^2)$ (dashed line) and $\mathrm{Re}T_{\sigma'}(q^2)$ (solid line). These curves have the following features. There are two zeros of $T_\sigma(q^2)$ for which the curve rises from negative values to positive values. These zeros correspond to resonances which we denote as σ_1 and σ_2. The values of $T_\sigma(q^2)$ exhibit strong cusp behavior at $q^2\simeq 4m_\pi^2$. Note also that $T_{\sigma'}(q^2)$ has no resonances in the range shown, since the states that we may call σ_3 and σ_4 are now are at higher energies.

In Fig. 12 we show $\mathrm{Im}T_\sigma(q^2)$ (dashed line) and $\mathrm{Im}T_{\sigma'}(q^2)$ (solid line). Again, strong cusp behavior is only seen in $\mathrm{Im}T_\sigma(q^2)$. The state σ_1 at $q^2=1.00\ \mathrm{GeV}^2$ has a large width and the width is quite asymmetric due to its proximity to the region of strong cusp behavior. The state σ_2 has a relatively narrow width and the T matrix could be well approximated by the form

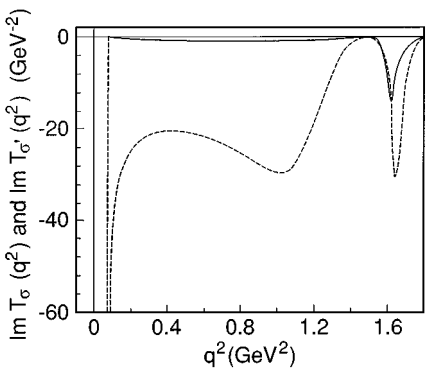

FIG. 12. The figure shows $\mathrm{Im}T_\sigma(q^2)$ (dashed line) and $\mathrm{Im}T_{\sigma'}(q^2)$ (solid line).

$$T_\sigma(q^2)=\frac{g^2}{q^2-m^2+im\Gamma}, \tag{6.1}$$

with $m^2=1.63\ \mathrm{GeV}^2$, $\Gamma=0.033$ GeV, and $g^2=1.35$. The small value of g^2 means that this state is only weakly coupled to quarks. In case of the broad asymmetric resonance at $q^2=1.00\ \mathrm{GeV}^2$, we can ask what the resonance parameters would be in the case the behavior below $q^2=1.00\ \mathrm{GeV}^2$ was modified so as to make the resonance symmetric. In that case, we would have $\Gamma=0.355$ GeV and $g^2=10.6$; however, a symmetric form does not provide a good representation of $T_\sigma(q^2)$. [See Fig. 12.]

VII. DYNAMICAL ORIGIN OF AN EFFECTIVE LOW-MASS SCALAR MESON FOR NUCLEAR PHYSICS

In this work we have seen that the σ_1 and σ_2 mesons have masses of 1 GeV or greater. Therefore, it appears that the σ_1 meson cannot be identified with the low-mass scalar ($m_\sigma\simeq 550$ MeV) often used in the description of the nucleon-nucleon interaction that is based upon the one-boson-exchange model [12]. In addition, a low-mass scalar plays an important role in the Walecka model [17] and in relativistic Brueckner-Hartree-Fock theory [18].

There is also a body of work that relates the mean σ field in nuclei to an order parameter for partial restoration of chiral symmetry at finite baryon density [19–22]. In that work the mean scalar field is related to the value of the quark condensate in matter. The reduction of the condensate in matter satisfies a well-known model-independent relation

$$\langle\overline{qq}\rangle_\rho=\langle\overline{qq}\rangle_0\left(1-\frac{\sigma_N\rho}{m_\pi^2 f_\pi^2}\right), \tag{7.1}$$

to first-order in the baryon density ρ. In Eq. (7.1), σ_N is the pion-nucleon sigma term whose value is usually given as $\sigma_N=45\pm 8$ MeV, and $\langle\overline{qq}\rangle_0$ is the vacuum value of the condensate. Thus, the reduction of the condensate is about 35% in nuclear matter. That is similar to the reduction of the nucleon mass from its vacuum value as seen in the Walecka model [17]. If one argues that the nucleon mass is (approximately) proportional to the value of the quark condensate, a fairly consistent picture emerges, with the mean scalar field being an order parameter for the deviation of the condensate from its vacuum value.

In the present work we wish to show how an *effective* low-mass σ meson emerges from our study of the quark-quark T matrix of the generalized NJL model. To study this matter, we first consider Eq. (6.1), which may be used to parametrize the $T_\sigma(q^2)$ component of the T matrix, if we make Γ q^2-dependent. We stress that, since m_σ is about 1 GeV in that parametrization, that form is only appropriate for large q^2. However, in nuclear physics studies the exchanged mesons are *spacelike* ($q^2\leqslant 0$), so we may ask how $T_\sigma(q^2)$ should be parametrized in the spacelike region. With reference to Fig. 13, we see that inclusion of $\mathrm{Re}\,\hat{K}_S(q^2)$ when calculating $\det D(q^2)$ changes the behavior in a dramatic fashion.

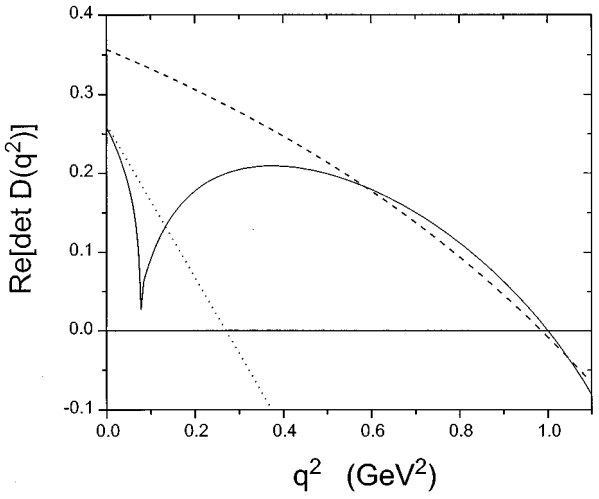

FIG. 13. The figure shows $\mathrm{Re}[\det D(q^2)]$. The solid line is the result obtained when including $\mathrm{Re}\hat{K}_S(q^2)$ and $\mathrm{Im}\hat{K}_S(q^2)$, as well as singlet-octet coupling. The dashed line is the result with $\hat{K}_S(q^2)=0$ and in the absence of singlet-octet coupling. The dotted line represents a linear approximation to $\mathrm{Re}[\det D(q^2)]$ (solid line) in the region $q^2\simeq 0$. For the dotted line, $\mathrm{Re}[\det D(q^2)]\simeq 0.97[(m_\sigma^{\mathrm{eff}})^2-q^2]$, with $m_\sigma^{\mathrm{eff}}=0.520$ GeV.

Note that for $q^2\leqslant 4m_\pi^2$, $\det D(q^2)$ is real. Near $q^2=0$, we may write $\det D(q^2)\simeq 0.97[(m_\sigma^{\mathrm{eff}})^2-q^2]$, with $m_\sigma^{\mathrm{eff}}\simeq 0.520$ GeV. That means that for small spacelike values of q^2, we can put

$$T_\sigma(q^2)\simeq\frac{(g_{\sigma qq}^{\mathrm{eff}})^2}{q^2-(m_\sigma^{\mathrm{eff}})^2}. \tag{7.2}$$

Inspection of Fig. 10 yields an approximate value of $g_{\sigma qq}^{\mathrm{eff}}=3.32$. Note that the strong q^2 dependence for small q^2 in $T_\sigma(q^2)$ is almost entirely due to the cusplike behavior of $\det D(q^2)$.

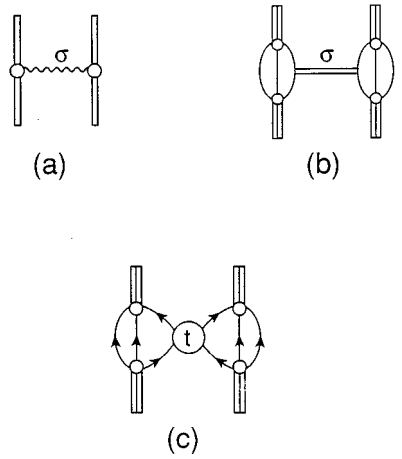

FIG. 14. (a) The one-boson-exchange (OBE) amplitude due to σ exchange between nucleons is shown. The circles denote the vertex cutoffs of the OBE model. (b) A representation of σ exchange in the NJL model based upon the use of a valence-quark nucleon form factor is shown. (c) The nucleon-nucleon interaction is related to a quark-quark T matrix. A σ-dominance model of the T matrix is shown in (b).

The T matrix for off-mass-shell quarks can be used in a model of the nucleon-nucleon force that is based upon that T matrix and valence-quark form factors of the nucleon. [See Fig. 14.] That model has been developed in a number of works [23–26]. Since the T matrix in the model considered here is parametrized by isoscalar-scalar exchange with $m_\sigma^{\rm eff} \simeq 520$ MeV, we see how we may understand one important feature of the boson-exchange model and of the Walecka model.

It is important to note that while inclusion of the cusplike behavior of $\mathrm{Re}\hat{K}_S(q^2)$ leads to a significant change when going from m_σ to $m_\sigma^{\rm eff}$, the value of $\det D(q^2)$ near $q^2=0$ is only reduced from its value in the absence of $\mathrm{Re}\hat{K}_S(q^2)$ by about 25%. That means that the predominant feature in scalar-isoscalar exchange in the nucleon-nucleon interaction is the exchange of the σ_1 meson, which we saw to be predominantly the $\sigma^0(1P)$ in our model.

VIII. DISCUSSION

In this work we have found two low-lying states that have energies of 1.00 and 1.28 GeV. The first of these states which we have denoted as σ_1, is predominantly the $\sigma^0(1P)$, while the state σ_2 is strongly mixed and has a rather small width for decay to two pions. Also, σ_2 is only weakly coupled to quarks. On the other hand, the state σ_1 is a quite broad and asymmetric resonance, as may be seen in Fig. 12. Clearly, coupling to the two-pion continuum is important over quite a broad range of energies for the σ_1. The situation is simpler for $q^2 \leqslant 4m_\pi^2$, where the T matrix is well approximated by the exchange of an *effective* σ meson that has a mass parameter $m_\sigma^{\rm eff} \simeq 520$ MeV. This small mass parameter has its origin in the cusplike behavior of $T_\sigma(q^2)$ at small q^2 which is due to the rapid opening of the two-pion channel.

We have identified the *effective* σ meson with the low-mass scalar that is extensively used in nuclear structure studies and studies of the nucleon-nucleon interaction. A schematic representation of the wave function of this scalar is $\sigma \simeq (\overline{uu}+\overline{dd}+\overline{ss})/\sqrt{3}$ in a first approximation. The consequences of this identification will be explored in a future work. In such future work, it should be possible to extend our analysis to an energy region beyond $q^2 = 1.8\ \mathrm{GeV}^2$. However, such an extension requires that we modify our procedure for calculation of the vacuum polarization diagrams $\hat{J}(q^2)$.

ACKNOWLEDGMENTS

This work has been supported in part by a grant from the National Science Foundation and by PSC-CUNY.

[1] L. S. Celenza, Xiang-Dong Li, and C. M. Shakin, Phys. Rev. C **55**, 3083 (1997).
[2] L. S. Celenza, C. M. Shakin, Wei-Dong Sun, J. Szweda, and Xiquan Zhu, Phys. Rev. D **51**, 3636 (1995).
[3] V. Bernard, R. L. Jaffe, and U.-G. Meissner, Nucl. Phys. **B308**, 753 (1988).
[4] T. Hatsuda and T. Kunihoro, Phys. Lett. B **185**, 304 (1987); **198**, 126 (1987).
[5] S. Klimt, M. Lutz, U. Vogl, and W. Weise, Nucl. Phys. **A516**, 429 (1990); U. Vogl, M. Lutz, S. Klimt, and W. Weise, *ibid.* **A516**, 469 (1990).
[6] M. Takizawa, Y. Nemoto, and M. Oka, Phys. Rev. D **55**, 4083 (1997).
[7] P. Rehberg, S. P. Klevansky, and J. Hüfner, Phys. Rev. C **53**, 410 (1996).
[8] U. Vogl and W. Weise, Prog. Part. Nucl. Phys. **27**, 195 (1991).
[9] S. P. Klevansky, Rev. Mod. Phys. **64**, 649 (1992).
[10] T. Hatsuda and T. Kunihiro, Phys. Rep. **247**, 223 (1994).
[11] C. M. Shakin and Wei-Dong Sun, Phys. Rev. C **55**, 614 (1997).
[12] R. Machleidt, in *Advances in Nuclear Physics*, edited by J. W. Negele and E. Vogt (Plenum, New York, 1989), Vol. 19.
[13] L. S. Celenza, Laiyu Li, Xiang-Dong Li, C. M. Shakin, and Wei-Dong Sun, Brooklyn College Report No. BCCNT 97/031/262, 1997 (unpublished).
[14] V. Dmitrašinović, Phys. Rev. C **53**, 1383 (1996).
[15] L. S. Celenza, Xiang-Dong Li, and C. M. Shakin, Phys. Rev. C **55**, 1492 (1997).
[16] Our method of performing momentum-space integral and only picking up the poles of the quark propagators is related to the scheme described in F. Gross and J. Milana, Phys. Rev. D **43**, 2401 (1991); **45**, 969 (1992).
[17] B. D. Serot and J. D. Walecka, in *Advances in Nuclear Physics*, edited by J. W. Negele and E. Vogt (Plenum, New York, 1986), Vol. 16.
[18] L. S. Celenza and C. M. Shakin, *Relativistic Nuclear Physics: Theories of Structure and Scattering* (World Scientific, Singapore, 1986).
[19] L. S. Celenza, B. Goulard, and C. M. Shakin, Phys. Rev. D **24**, 912 (1981).
[20] L. S. Celenza, A. Pantziris, C. M. Shakin, and Wei-Dong Sun, Phys. Rev. C **45**, 2015 (1992); **46**, 571 (1992).
[21] L. S. Celenza, C. M. Shakin, Wei-Dong Sun, and Xiquan Zhu, Phys. Rev. C **48**, 159 (1993).
[22] C. M. Shakin, Phys. Rev. C **50**, 1129 (1994).
[23] C. M. Shakin, Wei-Dong Sun, and J. Szweda, Phys. Rev. C **52**, 3353 (1995); **52**, 3502 (1995).
[24] L. S. Celenza, Shun-fu Gao, C. M. Shakin, Wei-Dong Sun, and J. Szweda, Phys. Rev. C **53**, 1936 (1996).
[25] L. S. Celenza, C. M. Shakin, and Wei-Dong Sun, Phys. Rev. C **54**, 487 (1996).
[26] C. M. Shakin and Wei-Dong Sun, Phys. Rev. C **55**, 614 (1997).